

## ESTIMATION OF MECHANOCHEMICAL EFFECTS IN HETEROGENEOUS PROCESSES

G. Mulas<sup>1,ξ</sup>, F. Delogu<sup>2</sup>

<sup>1</sup>Dipartimento di Chimica, Università di Sassari, via Vienna 2, I-07100 Sassari, Italy

<sup>2</sup>Dipartimento di Ingegneria Chimica e Materiali, Università di Cagliari, piazza d'Armi, I-09123 Cagliari, Italy

Keywords: Mechanochemistry, Heterogeneous processes, Kinetics

### Abstract

The present work focuses on the comparison of mechanochemical and thermal processes on a kinetic basis, with the aim of pointing out the higher efficiency of mechanically activated reactions in solid-solid, solid-liquid and solid-gas systems. The comparison relies upon the correlation between processing parameters, reaction kinetics and local deformation events. The obtained results are ascribed to the coupling of mechanical deformation with thermodynamic driving forces.

### Introduction

Mechanical processing promotes a significant enhancement of the chemical reactivity of solids in a number of inorganic and organic reaction systems [1-3]. Although a definite rationalization is still lacking [4-7], the complex phenomenology can be related to the intimate coupling of thermal and mechanical effects [8-11]. The systematic comparison of thermally and mechanically activated reactions represents a promising strategy to understand in more detail such aspects.

The present work, aimed at showing the potential of the above mentioned conceptual approach, focuses on the kinetics of solid-solid, solid-liquid and solid-gas mechanochemical transformations. The macroscopic and microscopic features of the system reactivity under mechanical processing are here compared with the ones exhibited by the same systems under thermal processing in order to point out mechanochemical effects and estimate their extent [12-15].

### Experimental Outline

Experiments were performed by employing a Spex Mixer Mill mod. 8000 and hardened-steel balls and vials. In the case of solid-gas reactions, the original Spex vial was replaced by an appositely manufactured reactor with the geometry but modified covers to permit the inlet and outlet of gases. The inelastic collision regime necessary to evaluate the average frequency and energy of collisions was attained by using a single ball and powder charges  $m_p$  of 8 g. Solid phase microstructure and thermal stability were investigated respectively by X-Ray diffraction (XRD) and differential scanning calorimetry. The specific surface area of processed powders was estimated by N<sub>2</sub> physical adsorption according to the BET method. Gases were analyzed by gas-chromatography. Full experimental details are reported elsewhere [12-17].

### Solid-Solid Mechanochemical Reactions

Ag and Cu are immiscible in the solid phase due to the relatively large positive heat of mixing [18]. Thus, thermal treatments are only able to produce alloys with a 2% terminal mutual solubility [18] unless very high cooling rates are imposed [2,19,20]. In contrast, the mechanical processing induces the formation of a metastable chemically-disordered Ag<sub>50</sub>Cu<sub>50</sub> solid solution [19-21]. The mechanochemical dissolution proceeds gradually *via* the formation of intermediate Ag- and Cu-rich solid solutions, the composition of which changes with the number  $n$  of collisions [21].

The mass fraction  $\alpha$  of the various phases is shown in Fig. 1. The analysis of kinetic curves at small  $n$  values points out that the first impact induces the formation of the Ag<sub>89</sub>Cu<sub>11</sub> and Ag<sub>12</sub>Cu<sub>88</sub> [21]. It is here worth noting that this and the successive compositional modifications should be ascribed to a shear-induced mixing of elemental species [22] and not to local melting processes followed by rapid cooling. In fact, these would form a Ag<sub>50</sub>Cu<sub>50</sub> alloy since the first impact.

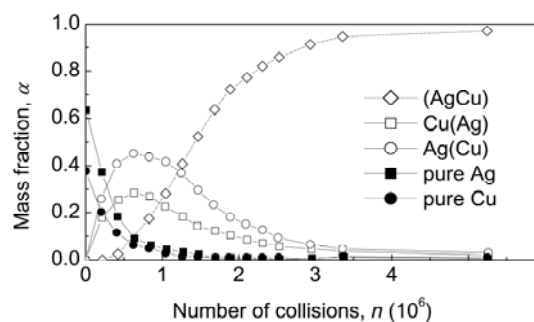


Figure 1. The mass fraction  $\alpha$  of the initial Ag and Cu reactants, of the intermediate Ag(Cu), and Cu(Ag) solid solutions and of the final (AgCu) solid solution as a function of the number  $n$  of collisions. Best-fitted curves are also shown [21]

Experiments with Co<sub>50</sub>Fe<sub>50</sub> binary mixtures provide a measure of the higher efficiency of shear-induced mixing compared to thermal diffusion. The progressive mechanochemical dissolution of Co into Fe determines the formation of a chemically-disordered solid solution [17]. The fraction  $\alpha$  of Co dissolved in Fe is given by the equation  $\alpha = \alpha_0 e^{-kn}$ , where  $\alpha_0$  is the initial Co mass fraction and  $k \approx 3.4 \times 10^{-7}$  is the apparent rate constant for Co dissolution.

<sup>ξ</sup> email: mulas@uniss.it

At the first impact, such amount is equal to  $\Delta\alpha \approx -\alpha_0 k$ . This corresponds to a number of Co atoms

$$N_{Co,mech} \approx \Delta\alpha m_p N_{Av}/M_{Co},$$

where  $M_{Co}$  is the Co atomic weight and  $N_{Av}$  the Avogadro number, of about  $2.81 \times 10^{16}$ . These dissolve into Fe in a time interval roughly equal to the impact duration  $\tau \approx 1$  ms [14,23]. Being the mass  $m^*$  of powder trapped at impact equal to about 1 mg [14,23], the mass  $m_{Fe}^*$  of Fe powder trapped at each impact is roughly equal to 0.49 mg. Since the Fe specific surface area  $S_{p,Fe}$  is roughly equal to  $12.3 \text{ m}^2 \text{ g}^{-1}$ , the maximum Fe surface area

$$S_{Fe} = S_{p,Fe} m_{Fe}^*$$

available to Co dissolution at the first impact amounts to about  $5.9 \times 10^{-3} \text{ m}^2$  [17]. The flux  $N_{Co,mech}/S_{Fe}\tau$  of Co atoms is then equal to about  $4.8 \times 10^{31}$  at  $\text{m}^2 \text{ s}^{-1}$  [17]. A simplified Boltzmann-Matano analysis [21,24] suggests that the number  $N_{Co,th}$  of Co atoms dissolving into Fe under thermal activation, referred to the same time interval  $\tau$  and interface area  $S_{Fe}$ , is comparable to  $N_{Co,mech}$  only at temperatures of 1000 K. Thus, the room temperature mechanochemical process is orders of magnitude faster than the thermal one.

### Solid-Liquid Mechanochemical Reactions

The conversion of acetone ( $\text{CH}_3\text{COCH}_3$ ) to 2-propanol ( $\text{CH}_3\text{CHOHCH}_3$ ) was studied by dispersing the liquid reactant on  $\text{Cu}_{40}(\text{MgO})_{60}$  catalyst powders [25] and submitting the system to mechanical processing. Full experimental procedures are given elsewhere [25].

The number  $\chi_{ac}$  of  $\text{CH}_3\text{COCH}_3$  moles is reported in Fig. 2 as a function of the number  $n$  of collisions. Data arrange according to a sigmoidal trend with a linear initial portion. The number  $\Delta\chi_{ac}$  of  $\text{CH}_3\text{COCH}_3$  moles reacted at the first impact amounts to about 2.1 nmol. Such quantity must be related to the impact duration  $\tau \approx 1$  ms and to the mass  $m_{Cu-Mg}^* \approx 1$  mg of catalyst powder processed at impact. The conversion rate  $\Delta\chi_{ac}/\tau m_{Cu-Mg}^*$  roughly amounts to  $2.1 \times 10^{-3} \text{ mol g}^{-1} \text{ s}^{-1}$ . Although this value is close to the one of  $4.4 \times 10^{-3} \text{ mol g}^{-1} \text{ s}^{-1}$  obtained under conventional flux conditions over the same  $\text{Cu}_{40}(\text{MgO})_{60}$  catalyst at a temperature of about 550 K [26], it must be noted that the mechanochemical reaction produces selectively  $\text{CH}_3\text{CHOHCH}_3$ .

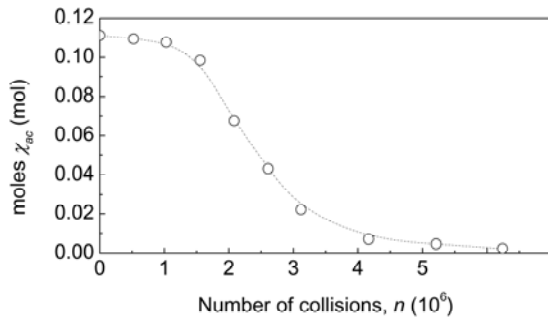


Figure 2. The number  $\chi_{ac}$  of  $\text{CH}_3\text{COCH}_3$  moles as a function of the number  $n$  of collisions. The dotted curve is a guide to the eye

### Solid-Gas Mechanochemical Reactions

The absorption of  $\text{H}_2$  by  $\text{Mg}_2\text{Ni}$  powders progressively induces the formation of a hydride phase [15]. The number  $\chi_s$  and  $\chi_d$  of  $\text{H}_2$  moles absorbed respectively under thermal and mechanochemical conditions are shown in Fig. 3 as a function of the processing time  $t$ .

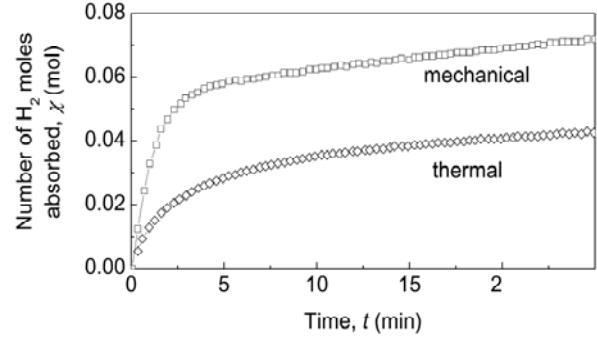


Figure 3. The number  $\chi_s$  and  $\chi_d$  of  $\text{H}_2$  moles absorbed under thermal and mechanical activation as a function of the time  $t$ . Best-fitted curves area also shown [15].

The most immediate evidence is that  $\chi_d$  is always larger than  $\chi_s$ . Absorption is satisfactorily described by the equation

$$\chi = \chi_f Kt/(1+Kt)$$

where  $\chi_f$  and  $K$  are respectively the final asymptotic number of  $\text{H}_2$  moles absorbed and the apparent rate constant for the sorption process [15]. At very short times  $\chi \approx \chi_f Kt$ . The equations above can be referred to both thermal (subscript  $s$ ) and mechanochemical (subscript  $d$ ) processes. The best-fitted  $\chi_{s,f}$  and  $K_s$  values amount to about 39 mmol and  $7.7 \times 10^{-3} \text{ s}^{-1}$ , whereas the values for  $\chi_{d,f}$  and  $K_d$  are 77 mmol and  $1.2 \times 10^{-2} \text{ s}^{-1}$ . The number  $\chi_{d,\tau}$  of  $\text{H}_2$  moles absorbed at the first impact, i.e. during a time interval  $\tau \approx 1$  ms, is equal to about 0.92  $\mu\text{mol}$ . The corresponding number of  $\text{H}_2$  moles  $\chi_{s,\tau}$  absorbed under thermal activation amounts instead to 0.3  $\mu\text{mol}$ . The difference could be motivated by a surface area increase due to the fragmentation of the powder particles at the impact. The specific surface area  $S_{p,\text{Mg}_2\text{Ni}}$  of  $\text{Mg}_2\text{Ni}$  powders and the mass  $m^*$  involved in impacts are equal to about  $15 \text{ m}^2 \text{ g}^{-1}$  and 1 mg respectively. The surface area  $S_{\text{Mg}_2\text{Ni}}$  available at the impact would then change from  $1.5 \times 10^{-2}$  to  $4.5 \times 10^{-2} \text{ m}^2$ . However, the  $\text{Mg}_2\text{Ni}$  powders employed were already submitted to a prolonged mechanical treatment, so that no change in surface area can be actually expected. It follows that the enhanced  $\text{H}_2$  absorption capability of  $\text{Mg}_2\text{Ni}$  powders should be ascribed to the formation of new highly reactive surface sites.

### Solid-gas Mechanochemical Catalysis

The reaction of CO and  $\text{H}_2$  was performed over a nanostructured  $\text{Co}_{50}\text{Fe}_{50}$  catalyst supported on  $\text{TiO}_2$  anatase in stoichiometric ratio 0.2 to 99.8 [27]. The number  $\chi_{CO}$  of reacted CO moles is shown in Fig. 4 as a function of the number  $n$  of collisions.

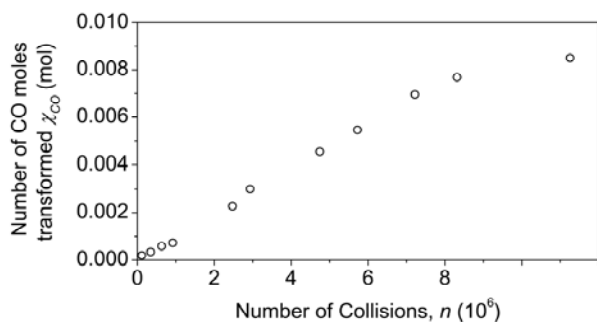


Figure 4. The number  $\chi_{CO}$  of CO moles reacted as a function of the number  $n$  of collisions

The mechanochemical reaction exhibits high selectivity to methane ( $\text{CH}_4$ ) and attains the maximum rate of about 0.94 nmol of CO transformed per impact, i.e.  $5.7 \times 10^{14}$   $\text{CH}_4$  molecules produced per impact, after about  $3.1 \times 10^6$  collisions [27]. With reference to the impact duration  $\tau \approx 1$  ms, the rate  $r$  of  $\text{CH}_4$  production amounts approximately to  $5.7 \times 10^{17}$  molec  $\text{s}^{-1}$  [27]. When CO and  $\text{H}_2$  are reacted over a similar catalyst under thermal activation [28], a conversion  $c$  of about  $13.8 \times 10^{-3}$  CO molec  $\text{s}^{-1}$  per active site is observed. The number  $S_{act}$  of active sites necessary to produce, under thermal activation, the CO conversion rate  $r$  observed under mechanical activation conditions is equal to  $r/c \approx 4.1 \times 10^{19}$  [28]. As a rough approximation, the active sites correspond to the number of Co and Fe surface atoms. Being the average  $\text{Co}_{50}\text{Fe}_{50}$  surface atomic density  $\rho$  equal to about  $1.6 \times 10^{19}$  at  $\text{m}^{-2}$  [29], the surface area  $S^* \approx S_{act}/\rho$  involved in the CO conversion processes at each impact amounts to about 2.5  $\text{m}^2$ . This value must be referred to the mass  $m^*_{\text{CoFe}}$  of the active  $\text{Co}_{50}\text{Fe}_{50}$  catalyst phase involved at each collision, roughly equal to 2.9  $\mu\text{g}$ . It follows that the supported  $\text{Co}_{50}\text{Fe}_{50}$  phase should have a specific surface area  $S^*/m^*_{\text{CoFe}}$  of about  $8.6 \times 10^5$   $\text{m}^2 \text{g}^{-1}$ . However, BET methods indicate that the specific surface area of the conventional and mechanically processed catalyst powders amounts to about 46 and 76  $\text{m}^2 \text{g}^{-1}$  [27]. Thus, the enhancement of catalytic activity under mechanical treatment conditions should be ascribed to a corresponding enhancement of the chemical reactivity of surface sites. Further calculations indicate that a mechanically activated surface site can be roughly  $1 \times 10^4$  to  $1 \times 10^6$  times more effective than a surface site under thermal activation [30].

#### Possible Atomic-Scale Mechanisms

Theoretically predicted or numerically inferred atomic-scale mechanisms are based on interface roughening and shear-induced disordering [8-11,21,22]. Although thermal diffusion is still regarded as an important component, the key role is played by atomic displacements induced by shear [8-11,21,22]. In fact, severe mechanical loads produce a series of localized shear events accompanied by the concentration of considerable amounts of energy in relatively small regions [8-11,21,22]. Shear-induced rearrangements generate defective atomic aggregates and mediate mass transport and chemical mixing [8-11,21,22]. As soon as the load is removed, shear events stop and transient defective structures relax, possibly disappearing due to thermal equilibration [8-11,21,22]. All of this suggests a strong coupling between thermally and mechanically induced mechanisms of mass transport, establishing a connection between the conventional

thermal diffusion scenarios and more recent approaches. Accordingly, mechanochemical phase transformations can be thought to originate from the competition of so-called ballistic displacements and thermal effects [8-11,21,22]. The same effects can be thought to operate in the case of surface-mediated processes such as absorption and catalysis, where the local destabilization of surface structures can result in a significantly enhanced reactivity. Also in this area, molecular dynamics methods are going to provide significant evidences of the intertwined processes of surface excitation and chemical conversion, as schematically shown in Fig. 5 [31]. In fact, higher conversion rates are obtained in the case of deforming surfaces [31].

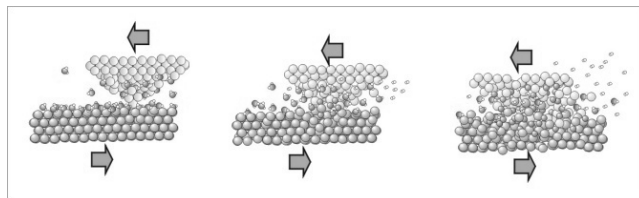


Figure 5. The chemical interaction of gaseous species at the point of contact between two sliding surfaces

#### Conclusions

Mechanochemical transformations exhibit a considerably larger efficiency when compared to similar thermally activated processes. Differences can amount even to several orders of magnitude when the kinetics of the mechanochemical reactions is suitably related to fundamental milling parameters. Such results cannot be ascribed to surface area effects, but rather should be regarded as a consequence of the local chemical reactivity enhancement due to energetic deformation events.

#### Acknowledgements

The University of Sassari and the University of Cagliari are acknowledged for financial support.

#### References

1. G. Heinicke, *Tribochemistry*, Akademie-Verlag, Berlin (1984).
2. C. Suryanarayana, *Prog. Mater. Sci.*, 46 (2001) 1.
3. B. Rodriguez, A. Bruckmann, T. Rantanen, and C. Bolm, *Adv. Synth. Cat.*, 349 (2007) 2213.
4. P.Yu. Butyagin, *Sov. Sci. Rev. B Chem.*, 14 (1989) 1.
5. B.B. Khina B B and F.H. Froes, *J. Met.*, 48 (1996) 36.
6. F.Kh. Urakaev V.V. and Boldyrev, *Powder Tech.*, 107 (2000) 93.
7. E.M. Gutman, *Mechanochemistry of Materials*, Cambridge International Science Publishing, Cambridge (1998).
8. V.I. Levitas, *Phys. Rev. B*, 70 (2004) 184118.
9. V.I. Levitas, *Phys. Rev. Lett.*, 95 (2005) 075701.
10. S.S. Sheiko *et al.*, *Nature*, 440 (2006) 191.
11. C.R. Hickenboth *et al.*, *Nature*, 446 (2007) 423.
12. F. Delogu *et al.*, *Int. J. Non-Eq. Proc.*, 11 (2000) 235.
13. F. Delogu, L. Schiffini, and G. Cocco, *Phil. Mag. A*, 81 (2001) 1917.

14. F. Delogu, G. Mulas, L. Schiffini, and G. Cocco *Mater. Sci. Eng. A*, 382 (2004) 280.
15. G. Mulas, L. Schiffini, and G. Cocco, *J. Mater. Res.*, 19 (2004) 3279.
16. G. Mulas, F. Delogu, and G. Cocco, *J. Alloys and Compd.*, 473 (2009) 180.
17. S. Garroni, F. Delogu, G. Mulas, and G. Cocco, *Scripta Mater.*, 57 (2007) 964.
18. E.A. Brandes and G.B. Brook (eds.), *Smithells Metals Reference Handbook*, 7<sup>th</sup> ed., Butterworth-Heinemann, Oxford (1992).
19. S. Zghal *et al.*, *Acta Mater.*, 50 (2002) 4695.
20. S. Zghal, R. Twesten, F. Wu, and P. Bellon, *Acta Mater.*, 50 (2002) 4711.
21. F. Delogu, *Acta Mater.*, 56 (2008) 905.
22. S. Odunuga, Y. Li, P. Krasnochtchekov, P. Bellon, and R.S. Averback, *Phys. Rev. Lett.*, 95 (2005) 045901.
23. D. Maurice and T.H. Courtney, *Metall. Mater. Trans. A*, 27 (1996) 1973.
24. R.W. Cahn and P. Haasen P (eds.), *Physical Metallurgy*, 4<sup>th</sup> ed., Elsevier Science BV, Amsterdam (1996).
25. G. Mulas, S. Deledda, and G. Cocco, *Mater. Sci. Eng. A*, 267 (1999) 214.
26. M. Varga, A. Molnar, G. Mulas, M. Mohai, I. Bertoti, and G. Cocco, *J. Catal.*, 206 (2002) 71.
27. S. Garroni, *Sintesi di Fischer-Tropsch attivata per via meccanica su catalizzatori nanostrutturati*, Degree Thesis in Chemistry, University of Sassari, Sassari (2007).
28. D.J. Duvenhage and N.J. Coville, *Appl. Catal. A*, 153 (1997) 43.
29. J.R. Anderson, *Structure of metallic catalysts*, Academic Press Inc., London (1975).
30. F. Delogu, G. Mulas, and S. Garroni, *Appl. Catal. A*, 366 (2009) 201.
31. F. Delogu, unpublished results.